



HAL
open science

Absorption of a poroelastic material with lateral air gaps

Nicolas Dauchez, Benoit Nennig

► **To cite this version:**

Nicolas Dauchez, Benoit Nennig. Absorption of a poroelastic material with lateral air gaps. 41st International Congress and Exposition on Noise Control Engineering (Internoise 2012), Aug 2012, New York, NY, United States. hal-01544604

HAL Id: hal-01544604

<https://hal.science/hal-01544604>

Submitted on 21 Jun 2017

HAL is a multi-disciplinary open access archive for the deposit and dissemination of scientific research documents, whether they are published or not. The documents may come from teaching and research institutions in France or abroad, or from public or private research centers.

L'archive ouverte pluridisciplinaire **HAL**, est destinée au dépôt et à la diffusion de documents scientifiques de niveau recherche, publiés ou non, émanant des établissements d'enseignement et de recherche français ou étrangers, des laboratoires publics ou privés.



Absorption of a poroelastic material with lateral air gaps

Nicolas Dauchez^{a)}

Benoit Nennig^{b)}

Institut Supérieur de Mécanique de Paris (Supmeca)

3, rue Fernand Hainaut

93407 Saint-Ouen cedex, France

In order to reduce noise in automotive or aircraft cabins, sound absorbing materials such as polymer foams or fibrous materials are widely used. To be efficient, their thickness must be in relation with the acoustical wavelength, making them not suitable in the low frequency range. To overcome this limitation while reducing weight, multilayer architectures and inclusions involving air gap or impervious structures, may be used. Up to now, most of the proposed models dealing with inclusions are based on rigid frame modeling. This assumption is not valid in general applications where a coupling with the frame may be observed. The aim of this paper is to investigate both the effect of air inclusions on the sound absorption of a poroelastic material and oblique incidence. The studied configuration is based on a square based hexahedre foam sample surrounded by air gaps of constant thickness. Measurements, performed in an impedance tube, are compared with finite element predictions (Biot-Allard model). The influence of the incident angle on the absorption coefficient is addressed assuming a periodic architecture. It is shown that lateral air gaps may increase the absorption by acting on the coupled air/skeleton resonances of the sample.

1 INTRODUCTION

Sound absorbing materials such as polymer foams or fibrous materials are widely used for noise control. To be efficient, their thickness must be in relation with the acoustical wavelength, making them not suitable in the low frequency range. To overcome this limitation while reducing weight, multilayer architectures including air, impervious or porous screens and porous layers may be optimized^{1,2,3}. Another mean is considering a non homogeneous porous layer, made for

^{a)} email: nicolas.dauchez@supmeca.fr

^{b)} email: benoit.nennig@supmeca.fr

instance of air inclusions in a homogeneous porous matrix. These materials are commonly called double porosity materials (DPM). Homogenisation technique^{4,5} have been first used to derive analytical models showing the main trends. To consider more complex shapes, finite element method^{6,7} coupling air and porous media have to be considered.

All the aforementioned papers are based on rigid frame modeling of the porous matrix. This assumption is not valid in general applications where the motion of the frame may be observed^{8,9}. Another conventional assumption in such context is the normal incidence excitation. The effect of oblique incidence have been shown by Groby¹⁰ on rigid circular inclusions and by Nennig¹¹ with air inclusion assuming periodic medium and Floquet wave decomposition.

The aim of this paper is to investigate both the effect of air inclusions on the sound absorption of a poroelastic material and oblique incidence.

2 COMPUTATIONAL APPROACH

Consider the time-harmonic (with the convention $\exp(-i\omega t)$) scattering problem depicted on Fig. 1. The configuration consists of an unbounded medium showing some d_1 and d_3 periodicity respectively on \mathbf{e}_1 and \mathbf{e}_3 direction. The medium is backed by a rigid wall and surrounded by an unbounded fluid domain. It is composed of a poroelastic surrounded by lateral air gaps. We call Γ the interface between the fluid domain and the poroelastic medium. In the surrounding fluid domain as in the air gaps, the pressure p must satisfied the Helmholtz equation

$$\Delta p + k_0^2 p = 0 \quad (1)$$

where, k_0 denotes the air wavenumber. In the poroelastic body, the acoustic waves propagation are described by Biot's model in the (\mathbf{u}, p) formulation¹² or by Equivalent Fluid model^{1,9}.

The incident field is a pressure plane $p^{\text{inc}} = e^{i\mathbf{k}\cdot\mathbf{x}}$ the scatter in the \mathbf{k} direction defined by the inclination θ and azimuth φ of the spherical coordinate system. In this case, both the incident and the scattered field are pseudo-periodic (i.e. \mathbf{d} -periodic with a phase difference). Indeed, each physical variable (call it \mathbf{X}) satisfied the relation

$$\mathbf{X}(\mathbf{x} + \mathbf{d}, \omega) = \mathbf{X}(\mathbf{x}, \omega)e^{i\mathbf{k}\cdot\mathbf{d}}, \quad (2)$$

with $\mathbf{d} = (d_1, 0, d_3)$. This property allows substantial simplifications because only one elementary cell need to be meshed and permit to define properly the radiation condition thought a modal decomposition^{11,13}. This approach was preferred here as the use of the PML technique is not efficient for 'low-frequency' applications, i.e. when the wavelength is large compared to the size of the computational domain. The highest Floquet mode index taken in account in each direction is chosen as the number of cut-on Floquet mode + 1.

The FEM computations are carried out using Lagrange quadratic tetrahedral finite elements. The radiation condition of the scattered field in the upper air domain, is implemented with Dirichlet to Newman (DtN) map based on the Floquet decomposition. To apply easily the Floquet relation recalled in equation (2), coincident meshes on each opposite lateral boundary of the periodic cell are used^{14,15}. Unstructured mesh are employed in the remainder of the computational domain (Fig. 2). The characteristic element length is fixed in all cases to ensure 1 element in the air gap. This yields approximatively to 100 000 degrees of freedom FEM models.

The integration of the acoustic intensity relation over the unit cell using orthogonality the Floquet modes leads to the power balance. We define the power reflection coefficient R as the ratio of the scattered power in the \mathbf{e}_2 direction $P_r = \sum_{m,n \in \mathbf{Z}} \Re\{\beta_{m,n}\} |A_{m,n}| / (\rho_0 \omega)$ to the incident power $P_i = k_2 d / (\rho_0 \omega)$ with the vertical wavenumber $\beta_{m,n} = \sqrt{k_0^2 - \left(k_1 + m \frac{2\pi}{d_1}\right)^2 - \left(k_3 + n \frac{2\pi}{d_3}\right)^2}$ and $A_{m,n}$ the modal amplitude. Thanks to the conservation of the energy, the absorbed power is given by $P_{\text{abs}} = P_i - P_r$. In this way, we can define the absorption coefficient

$$\alpha = \frac{P_{\text{abs}}}{P_i} = 1 - R. \quad (3)$$

3 RESULTS

In this part, we consider the sound absorption of a porous sample with lateral air gaps of thickness h (Fig.1). The sample geometry is a square based hexahedre of lateral size $l_1 = 90$ mm and thickness $l_2 = 100$ mm. The material is an open cell polymer foam (properties in Tab. 1).

3.1 Influence of elastic frame at normal incidence

Experimental data are given at normal incidence¹⁶. The absorption is measured in an impedance tube using a two microphones technique. The tube has a square cross section of 100 mm side ($d_1 = d_3 = 100$ mm). The lateral air gaps thickness is $h = 5$ mm. This thickness may be modified by reducing the cross section of the duct (d_1 and d_3) by bonding non porous material (rubber) along the tube.

Figure 3 presents the absorption coefficient for several thicknesses: $h = 5$ mm, 1.8 mm or 0 mm. In the last case, the porous sample is in contact with the tube wall and can be considered as clamped (no vertical motion of the skeleton at boundary). Without air gap, the absorption coefficient increases slightly with frequency and a peak is observed around 300 Hz. It is related to a skeleton resonance of the porous sample. With an air gap, the absorption coefficient is globally better except in the lower and upper bound of the considered frequency range. Two peaks are observed this time. The first one is mainly related to a skeleton resonance while the second one to a fluid resonance. When decreasing the air gap from 5 mm to 1.8 mm, both peaks are shifted towards lower frequencies. The absorption is then better in the low frequency range with the 1.8 mm air gap.

Fig. 4 compares rigid and elastic frame models for a 5 mm and 1.8 mm thick air gap. The same trends are confirmed. Since the first peak is due to a frame resonance, it cannot be observed with the rigid frame model. Moreover, in the region of the second peak, the difference between both models increases when the air gap thickness decreases. In this region, not considering the frame as elastic may cause significant error in the location and amplitude of the maximum absorption coefficient.

3.2 Effect of oblique incidence

Let consider now the sound absorption at oblique incidence θ (φ is set to 0). Only theoretical results will be presented. In order to account for oblique incidence, a periodic arrangement has to be considered.

Fig. 5 shows the absorption coefficient at normal and oblique incidence of the same sample with 5 mm lateral air gap. The same trends are observed for both elastic and rigid frame models. The maximum decreases with the angle and is shifted towards high frequencies. The absorption becomes better in the low frequency range. The change is accelerating at higher incidence angle (i.e. between 60 and 80 degrees). Moreover, another peak arises at low frequency (around 76 Hz) near grazing incidence: it is related to the Biot shear wave. Note that the frequency of these two first peaks is not function of the angle. They both contribute to a significant increase of the absorption coefficient in the low frequency range in comparison with the rigid frame model.

4 CONCLUSION

The effect of lateral air gaps around a poroelastic material sample has been investigated for several angles of incidence. Both experiments and models show that air gaps may increase the absorption in the low frequency range. When the frame is considered as elastic, it is shown that additional absorption peaks are observed, linked to longitudinal or shear motion of the porous sample. Moreover, the location and the amplitude of the maximal absorption coefficient may not be accurately predicted with the rigid frame model.

Further works will deal with the influence of frame motion on the efficiency of light membrane inclusions that may amplify the phenomenon.

6 REFERENCES

1. J.F. Allard and N. Atalla, *Propagation of Sound in Porous Media*, John Wiley & Sons Ltd, Chichester, UK, (2009)
2. O. Tanneau, J. B. Casimir and P. Lamary, "Optimization of multilayered panels with poroelastic components for an acoustical transmission objective", *J. Acoust. Soc. of Am.*, **120**(3), (2006)
3. J. Kanfoud, M.A. Hamdi, F.X. Becot and L. Jaouen, "Development of an analytical solution of modified Biot's equations for the optimization of lightweight acoustic protection", *J. Acoust. Soc. of Am.*, **125**(2), (2009)
4. X. Olny, C. Boutin, "Acoustic wave propagation in double porosity media", *J. Acoust. Soc. Am.*, **114**(1), (2005)
5. E. Gourdon, M. Seppi, "On the use of porous inclusions to improve the acoustical response of porous materials: Analytical model and experimental verification", *Appl. Acoust.*, **71**(4), (2010)
6. N. Atalla, R. Panneton, F. C. Sgard, X. Olny, "Acoustic absorption of macro-perforated porous materials", *J. Sound Vib.*, **243**(4), (2001)
7. F. C. Sgard, X. Olny, N. Atalla, F. Castel, "On the use of perforations to improve the sound absorption of porous materials", *Appl. Acoust.*, **66**, (2005)

8. Doutres O., Dauchez N., G enevaux J.-M., Porous layer impedance applied to a moving wall: Application to the radiation of a covered piston, *J. Acoust. Soc. Am.*, **121**(1), 206-213, 200
9. Doutres O., Dauchez N., G enevaux J.-M., Dazel O., Validity of the limp model for porous materials: A criterion based on the Biot theory, *J. Acoust. Soc. Am.*, **122**(4), 1845-2476, 2007
10. J.-P. Groby, A. Wirgin, L. De Ryck and W. Lauricks, "Acoustic response of a rigid frame porous medium slab with a periodic set of inclusions", *J. Acoust. Soc. Am.*, **126**(1), (2009)
11. B. Nennig, Y. Renou, J.-P. Groby and Y. Auregan, "A mode matching approach for modeling two dimensional porous grating with infinitely rigid or soft inclusions", *J. Acoust. Soc. Am.*, **131**(5), (2012)
12. N. Atalla, R. Panneton and P. Debergue, "A mixed displacement-pressure formulation for poroelastic materials", *J. Acoust. Soc. Am.*, **104**(3), (1998)
13. C. M. Linton and I. Thompson, "Resonant effects in scattering by periodic arrays", *Wave Motion*, **44**(3), (2007)
14. A. Nicolet, S. Guenneau, C. Geuzaine and F. Zolla, "Modelling of electromagnetic waves in periodic media with finite elements", *J. Comput. Appl. Math.*, **168**(1-2), (2004)
15. A. Hennion, R. Bossut, J. Decarpigny and C. Audoly, "Analysis of the Scattering of a Plane Acoustic-Wave by a Periodic Elastic Structure Using the Finite-Element Method - Application to Compliant Tube Gratings", *J. Acoust. Soc. Am.*, **87**(5), (1990)
16. N. Dauchez, Etude vibroacoustique des mat eriaux poreux par  el ements finis, Ph. D. Thesis, University of Le Mans (France) and University of Sherbrooke (Canada), (1999)

Table 1 – Poroelastic material properties.

Porosity	0.97
Resistivity [Nm^{-4}s]	165 500
Tortuosity	1.8
Viscous length [μm]	60
Thermal length [μm]	180
Young's Modulus [Pa]	206 000
Poisson's Ratio	0.45
Loss Factor	0.11
Skeleton density [$\text{kg}\cdot\text{m}^{-3}$]	39.5

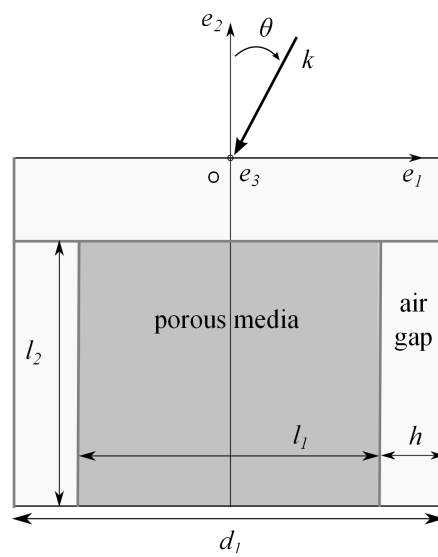


Fig. 1 – Model of the porous sample with lateral air gaps.

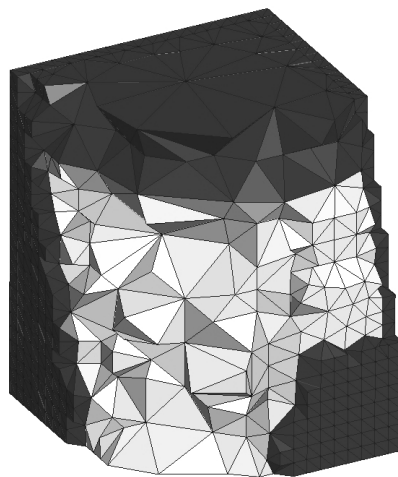


Fig. 2 – Mesh of the periodic cell.

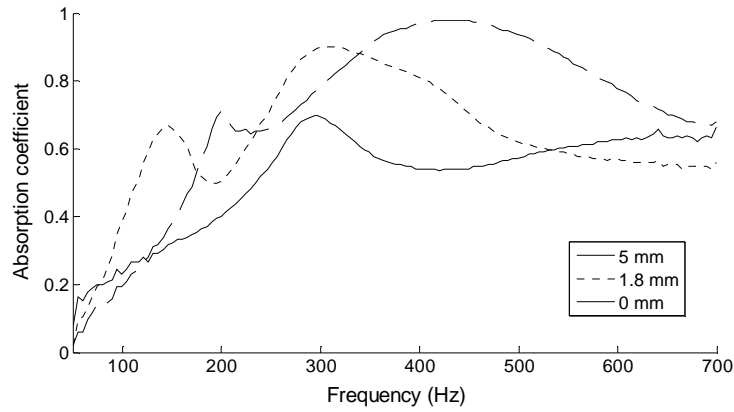


Fig. 3 – Measured absorption coefficient at normal incidence for several air gap thicknesses: (continuous line) $h=0$ mm, (dotted line) $h=1.8$ mm, (dashed line) $h=5$ mm.

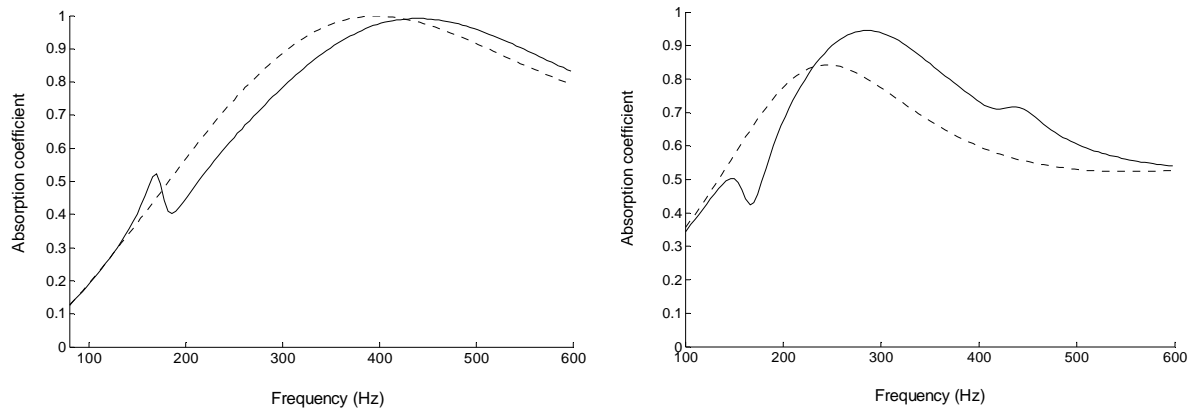


Fig. 4 – Simulated absorption coefficient at normal incidence for a 5 mm (left) and a 1.8 mm (right) lateral air gap: (continuous line) elastic frame, (dashed line) rigid frame.

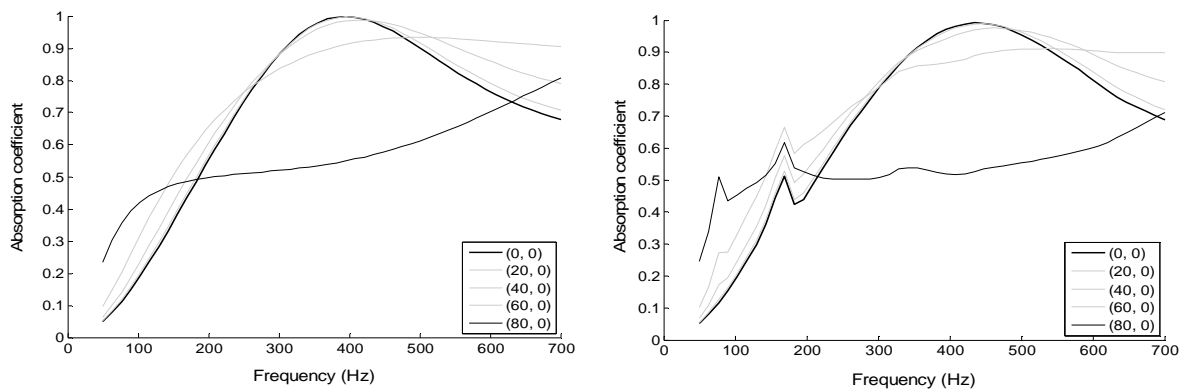


Fig. 5 – Simulated absorption coefficient at normal ($0, \varphi=0$) and oblique incidence ($20-80, \varphi=0$) of a sample with 5 mm lateral air gap: (left) rigid frame, (right) elastic frame.